

Kinetics of Ion Removal from an Iron-Rich Industrial Coproduct: III. Manganese and Chromium

Yigal Salingar, Donald L. Sparks,* and John D. Pesek

ABSTRACT

An iron-rich material (IRM) contained the potential soil and water pollutants Mn and Cr. Therefore, to assess the feasibility of using the IRM in agricultural and nonagricultural settings, this study was conducted to determine the processes and kinetics of Mn and Cr (total soluble metals) retention and removal from the IRM. This was accomplished by employing adsorption isotherms, column studies, and the stirred-flow (SF) kinetic technique. Manganese adsorption conformed to the Langmuir equation and Cr adsorption was described by the Freundlich equation. The kinetic studies showed that indigenous Mn salts were depleted instantaneously via a volume-dependent process. Both Mn and Cr in the IRM became solubilized while being processed at the industrial plant. But, unlike Mn, Cr was reabsorbed by the IRM after the initial solubilization. This fraction of the Cr was desorbed rapidly, conforming to first-order kinetics and yielding a rate-constant of 0.56 min^{-1} . After the rapid removal of some of the Mn and Cr, a steady-state with wadginite may have governed Mn removal, and chromite may have controlled the Cr concentration, through zero-order dissolution reactions. Both column and SF studies showed that the proportion of total soluble (dischargeable) Mn and Cr was small.

Y. Salingar, Soil Reclamation Dep., Keren Kayemeth LeIsrael, P.O. Box 45, 26103 K. Hayim, Israel; and D.L. Sparks and J.D. Pesek, Dep. of Plant and Soil Sci., University of Delaware, Newark, DE 19717-1303. Received 20 Oct. 1992. *Corresponding author (dlsparks@brahms.udel.edu).

Published in J. Environ. Qual. 23:1205-1211 (1994).

A TiO_2 MANUFACTURING PROCESS produces an iron-rich industrial coproduct. Physicochemical characterizations of this filter-cake material along with the mechanism and kinetics of Cl and SO_4 removal are given elsewhere (Salingar et al., 1994a,b). A recent study concluded that the IRM may be suitable for agricultural uses (Goyette, 1992). It contained, however, Mn and Cr in concentrations high enough to be potential pollutants of soil and water. Chromium (VI) can be toxic to mammals, and the hazard of Cr^{3+} is its potential oxidation to Cr^{6+} . The objectives of this study were (i) to determine Mn and Cr retention and removal characteristics from the IRM, and (ii) to ascertain the kinetics of Mn and Cr removal from the IRM.

Manganese-oxide and hydroxide minerals contain Mn^{2+} , Mn^{3+} , and Mn^{4+} . In soils, some of these ions may be reduced or oxidized. Manganese adsorbs on most charged surfaces and coprecipitates with most hydrolyzable cations (McKenzie, 1989). In aqueous systems, Mn^{3+} is unstable compared with Mn^{2+} . Manganese²⁺ is mobile, whereas Mn^{3+} and Mn^{4+} tend to precipitate oxides or hydroxides (Baes and Mesmer, 1976).

Abbreviations: CEC, cation-exchange capacity; CV, the coefficient of variation; EC, electrical conductivity; IRM, iron-rich material; NLLS, nonlinear least squares; ODE, ordinary differential equations; SF, stirred-flow technique.

Shuman (1977) found that Mn adsorption data conformed to the Langmuir isotherm, and Stuanes (1976) showed that there is good agreement between the adsorbed quantity of Mn and the cation-exchange capacity (CEC) of clay minerals. Sadiq (1981) reported a correlation between Mn sorption and various properties (not including CEC) of 27 different mineral soils. Some Cl salts (KCl, NaCl, and CaCl₂) increased the Mn availability and exchangeable Mn levels in soils. Krishnamurti and Huang (1988) found that deionized-distilled water and KCl effected appreciable release of Mn from selected Mn-oxide minerals. The Mn release increased with increasing concentration of KCl.

There are few reports in the literature on the kinetics of Mn reactions in soils and on soil constituents (Sparks, 1989). Krishnamurti and Huang (1988) found that Mn release from selected Mn-oxide minerals using KCl was initially rapid and then decreased, following multiple zero-order kinetics.

Chromium concentrations in the environment are often high because of the heavy industrial use of Cr. Its oxidation states range from -2 to +6, but only Cr³⁺ and Cr⁶⁺ are stable under surface conditions and in the Eh and pH range normally found in soils. There are similarities between Cr³⁺ and Fe³⁺ (Grove and Ellis, 1980), and Cr³⁺ and Al³⁺ chemistry in soils (Bartlett and James, 1979). The solubility of Cr³⁺ in soils is often controlled either by Cr³⁺ coprecipitated with Fe-oxides and hydroxides or by Cr(OH)₃ (s). Hydrolysis constants and a solubility product for Cr(OH)₃ (s) were recently revised by Rai et al. (1987). Elemental Cr is not found in nature; chromite, (Fe, Mg) O (Cr, Al, Fe)₂O₃, is the only important commercial Cr ore (Rollinson, 1973).

Chromium⁶⁺ is more hazardous than Cr³⁺ because it is a carcinogen, an irritant, and corrosive (National Academy of Science, 1974). Additionally, Cr⁶⁺ is more mobile in many soil and water systems than most other cations, whereas Cr³⁺ is less mobile because of its limited solubility as hydroxide, sorption on negatively charged surfaces in soils and sediments, and complexation with insoluble organic matter. In most soils, Cr⁶⁺ is reduced by organic matter, Fe²⁺ and sulfides. Low soil pH favors rapid reduction of Cr⁶⁺ (Griffin et al., 1977; Grove and Ellis, 1980). El-Bassam et al. (1975) reported that applied Cr⁶⁺ was not leached from soil columns because it was reduced to Cr³⁺.

Chromium³⁺ can be a hazard if it oxidizes to Cr⁶⁺. The only common naturally occurring oxidizing agents of Cr³⁺ are Mn-oxides, and O₂ when the pH is >9 (Bartlett and James, 1979). The extent of Cr³⁺ oxidation under typical environmental conditions, however, did not exceed 15% of the initial Cr³⁺ present (Saleh et al., 1989). As pH and Cr³⁺ concentration increased, Cr³⁺ oxidation was limited (Amacher and Baker, 1982), and a surface alteration mechanism appears to account for the decreasing oxidation rates and oxidation inhibition (Fendorf and Zasoski, 1991). Direct physical evidence showed that a Cr(OH)₃ nH₂O surface precipitate was formed. It inhibits a Cr³⁺ oxidation by acting as a redox-stable sink for Cr³⁺, and establishes a physical barrier

between solution Cr³⁺ and the oxidative MnO₂ surface (Fendorf et al., 1992).

There is little information about Cr³⁺ sorption on soils. Griffin et al. (1977) studied a municipal landfill leachate and found that kaolinite and montmorillonite adsorbed ≈ 30 to 300 times more Cr³⁺ than Cr⁶⁺. In contrast to Griffin et al. (1977), Grove and Ellis (1980) suggested that only reduction to the insoluble forms of Cr³⁺, and no adsorption, accounted for the disappearance of added soluble Cr⁶⁺ from solution.

Few reports exist on the kinetics of Cr reactions in soils and on soil constituents (Sparks, 1989). Amacher and Baker (1982) found that Cr³⁺ sorption on a silt-loam soil was too fast to measure using a batch technique. Amacher et al. (1986) found that first, second, and *n*th-order kinetic models failed to adequately describe the kinetics of Cr retention on soils. Later, Amacher et al. (1988) successfully employed a nonlinear multireaction model for predicting the kinetics of Cr⁶⁺ retention on various soils at several initial concentrations. Saleh et al. (1989) found that oxidation of Cr³⁺ by MnO₂, and reduction of Cr⁶⁺ by S²⁻ or Fe²⁺ are rapid, whereas Cr⁶⁺ reduction by organics in sediments and soils is slower and kinetically controlled.

MATERIALS AND METHODS

Characterization analyses of IRM samples along with detailed methodologies that were used in the column and the kinetics (stirred-flow) studies are given elsewhere (Salingar et al., 1994a,b). The Mn and Cr analyses are given in Table 1. In this study, Mn and Cr denoted total soluble metal. In the column study, using the Cr oxidation test of Bartlett and James (1979), it was found that all of the Cr in the column effluents was Cr³⁺, and Cr⁶⁺ was below the detection limit of the test.

The x-ray diffraction analyses (random powder mounts) indicated the presence of wadginitite, (Ta, Mn, Nb, Sn)O₂, (Card no. 31-838; JCPDS, 1986) in the IRM. Peaks were observed at 0.178, 0.295 and 0.251 nm, and weaker signals at 0.174, 0.193, and 0.187 nm. Three distinct peaks characteristic of a Fe-Cr oxide, with an intense peak at 0.252 nm, and weaker signals at 0.207 and 0.295 nm were also observed. These values agree with the *d*-spacing data for chromite-aluminian [Fe (Cr, Al)₂ O₄] (Card no. 3-873; JCPDS, 1986). The *d*-spacing of 0.147 nm for wadginitite and the two *d*-spacings of 0.160 and 0.146 nm for chromite were not detected since they were below the first *d*-spacing value we analyzed (0.173 nm).

Table 1. Electrical conductivity†, pH, Cr, and Mn concentrations in the iron-rich material (IRM).

	HF Digestion‡	XRF§	First leachate¶	SP#
	g kg ⁻¹		µg L ⁻¹	
EC	NA††	NA	4.3	1.59 ± 0.05
pH	NA	NA	7.17	6.55 ± 0.07
Mn	12.3	19.4	737	274 ± 17
Cr	1.67	2.3	2.9	9.5 ± 1.5

† EC is expressed in units of dS m⁻¹.

‡ Total digestion, modified from Bernas (1968): HF + HNO₃ + HClO₄ in a teflon bomb, at 378K for 12 h.

§ X-ray fluorescence (a semiquantitative analysis).

¶ The first effluent sample collected from the IRM column.

Saturated paste extraction. The gravimetric water content (ω) was 1.05 ± 0.04 (kg kg⁻¹).

†† NA means no data available.

Static Studies

Isotherm studies of Mn and Cr adsorption on IRM at 298 K were performed by continuously shaking 1 g IRM (air-dried, <2.0 mm) in 10 mL solution for 24 h (end-to-end on a reciprocating shaker). Preliminary studies indicated the reaction reached a steady state within 24 h and the solid/liquid ratio was arbitrarily chosen. These suspensions included 11 Mn solutions of initial concentrations (Mn_0) of 0 to 100 mg L⁻¹, and 11 Cr (Cr_0) solutions of 0 to 200 mg L⁻¹ in a background electrolyte of 0.01 M NaNO₃. Initial pH values were measured, the IRM was added, and to minimize precipitation pH was lowered and adjusted to 4.55 ± 0.04 using trace quantities of HNO₃ and NH₄OH. After a 24 h shaking period final pH values were measured, then the slurries were centrifuged ($30\,600 \times g$ for 30 min), filtered (0.45 μ m), and Mn and Cr were measured using inductively coupled plasma spectrometry. Detection limits of the inductively coupled plasma techniques were calculated based on: 3σ of the intensity of the blank, where σ is the standard deviation. Detection limits were 0.23 μ g L⁻¹ for Mn and 9.7 μ g L⁻¹ for Cr.

Kinetics (Stirred-Flow) Studies

The rate of Mn and Cr released from IRM was investigated using a stirred-flow (SF) technique described earlier (Salingar et al., 1994a). Air-dried IRM was loaded (200 mg) into the reaction chamber and 6.93 mL of 10 mM Ba (as BaCl₂) was added. This volume (V_{ch}) was maintained throughout the reaction period. The electrical conductivity (EC) of the eluent was 1.89 dS m⁻¹ and its pH was 5.58. A steady flow-rate (Q) of 3.37 ± 0.10 mL min⁻¹ was achieved by using a peristaltic pump, and the effluent fractions were collected at 0.58 ± 0.02 min intervals using a fraction collector. The effluent was analyzed for Mn and Cr as described earlier.

RESULTS

Adsorption Isotherms

The Mn adsorption isotherm (Fig. 1) conformed to the Langmuir equation. From the regression of the linear form of the Langmuir equation ($r^2 = 0.996$), K (a constant related somewhat to the binding strength) was 5.87×10^6 L kg⁻¹, and b (adsorption capacity) was 1.136 g kg⁻¹. Although the b value we calculated conformed with Shuman's (1977) findings (in four different soil samples b ranged from 0.05 to 1.06 g kg⁻¹) our predicted K did not. According to Shuman (1977) K ranged from 4.3×10^4 to 3.85×10^5 L kg⁻¹. The

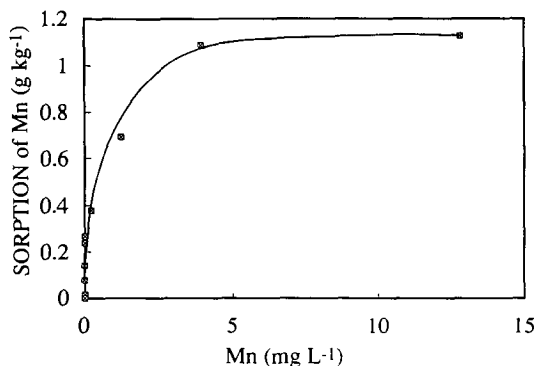


Fig. 1. Manganese adsorption isotherm for iron-rich material (IRM).

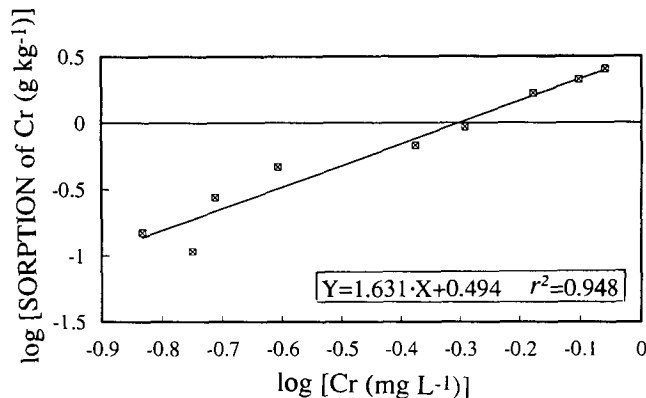


Fig. 2. Freundlich isotherm for Cr adsorption on iron-rich material (IRM).

findings in our study indicated a greater affinity of Mn for IRM than the affinity shown by the four soils studied by Shuman (1977).

The Cr adsorption data failed to conform to the Langmuir equation, but they did conform to the Freundlich equation (Fig. 2). The determined values for the empirical constants n and K were 0.613 (unitless) and 3.116×10^6 L kg⁻¹, respectively.

Column Studies

Manganese

A model of Mn concentration in the column effluent vs. pore volume (ρ) was fitted (Fig. 3) using nonlinear least squares (NLLS),

$$Mn = Mn_i \exp(-k_3\rho) + Mn_s \quad [1]$$

where Mn_i is initial Mn concentration in the column (μ g L⁻¹), Mn_s is replenished Mn in the column (μ g L⁻¹), and k_3 is a constant (ρ^{-1}). The term $Mn_i \exp(-k_3\rho)$ denotes the ρ -dependent instantaneously removed Mn fraction, and Mn_s is sustained by an infinite source. Further elucidations of M_i and M_s will be discussed

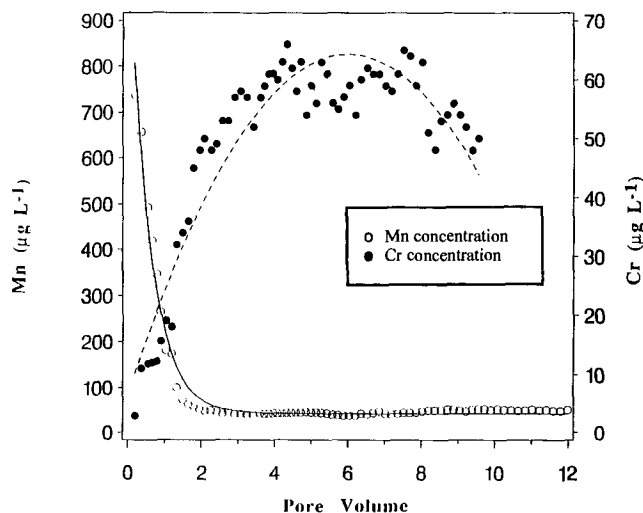


Fig. 3. Measured and fitted Mn concentration, and measured and fitted (broken line) Cr concentration vs. pore volume in the column.

below. Table 2 gives estimated values and coefficients of variation (CVs) for Mn_i , Mn_s , and k_3 , along with pseudo R^2 for the fit. Considering the dilution factor (measurements were taken only after ≈ 20 mL of effluent were collected), and extrapolating the Mn line in Fig. 3 to $\rho = 0$, the model estimation for Mn_i ($1071 \mu\text{g L}^{-1}$) was plausible. The evaluation for Mn_s ($42 \mu\text{g L}^{-1}$) agreed with the data that leveled off at $\approx 48 \mu\text{g L}^{-1}$. Setting the estimated values for Mn_i and k_3 in the term $[Mn_i \exp(-k_3\rho)]$ also showed good agreement with the data for $1.8 > \rho > 0$.

Chromium

The removal of Cr^{3+} showed a parabolic behavior vs. ρ (Fig. 3). A quadratic model, up to $\rho = 9.6$, was fitted ($R^2 = 0.88$),

$$\text{Cr} = 6.57 + 19.3\rho - 1.61\rho^2 \quad [2]$$

where the CV value for the intercept was 0.34, for the linear coefficient 0.055, and for the quadratic coefficient 0.066.

The maximum of the fitted parabolic curve was at 5.6ρ . Interpretation of the Cr leaching behavior will be discussed below.

Kinetics Studies

Model predictions, which are described below, were compared with experimental data collected from SF studies to verify the assumptions of the models. The employment of this approach allowed one to follow the time-dependent release of Mn and Cr in a heterogenous-complex system, for which other modeling approaches would require non-obtainable information on specific sites and sources of the released species.

As discussed earlier (Salingar et al., 1994a), estimation of model parameters by best fit to experimental data, and not by independent measurements, may lead to erroneous conclusions. Thus, in the SF studies given below, the parameter ξ (the reciprocal of the chamber volume, V_{ch}), and the parameters M_{0,Mn_i} (initial mass of instantaneously-removed Mn) and M_{0,Cr_i} (initial mass of rapidly-removed Cr) were determined directly from the data and compared with the values estimated by the models.

Modeling the Manganese Removal

After ≈ 24 min, at the end of the SF experiment, most salts were leached; EC in the chamber equaled the EC in the eluent (1.89 dS m^{-1}).

To establish Mn modeling, the following setup of

Table 2. Estimated parameters for the model of Mn concentration vs. pore volume (ρ) in the column (Eq. [1]).†

Parameter	Estimated	Coefficient of variation	Pseudo R^2
$Mn_i, \mu\text{g L}^{-1}$	1071	0.028	0.98
$Mn_s, \mu\text{g L}^{-1}$	42	0.055	
k_3, ρ^{-1}	1.77	0.032	

† Mn_i is initial Mn mass in the solution; Mn_s is replenished Mn mass in the solution; k_3 is a constant.

ordinary differential equations (ODEs) was proposed for the SF system:

$$\frac{dM_{Mn_s}}{dt} = k_4 - \tau_2 \quad M_{Mn_s} = 0 \text{ when } t = 0 \quad [3]$$

where $\tau_2 = \xi M_{Mn_s} Q$

$$\frac{dM_{ac,Mn_s}}{dt} = \tau_2 \quad M_{ac,Mn_s} = 0 \text{ when } t = 0 \quad [4]$$

$$\frac{dM_{ac,Mn_i}}{dt} = \tau_3 \quad M_{ac,Mn_i} = 0 \text{ when } t = 0 \quad [5]$$

where $\tau_3 = \xi M_{Mn_i} Q$, and $M_{Mn_i} = M_{0,Mn_i} - M_{ac,Mn_i}$

$$\frac{dM_{ac,Mn_{tot}}}{dt} = \xi (M_{Mn_s} + M_{Mn_i}) Q$$

$$M_{ac,Mn_{tot}} = 0 \text{ when } t = 0 \quad [6]$$

where t is time (min), M_{Mn_s} is current mass (M) of slowly-removed Mn in solution in the chamber (μg), M_{ac,Mn_s} is accumulated Mn_s removed from the chamber (μg), k_4 is a rate-constant for Mn_s entering the solution ($\mu\text{g min}^{-1}$), τ expressions denote sink terms as implied by the SF methodology, $\xi = V_{\text{ch}}^{-1}$ (0.144 mL^{-1}) in which V_{ch} is volume of the chamber (6.93 mL), Q is flow-rate (mL min^{-1}), M_{Mn_i} is current mass of instantaneously removed Mn in solution in the chamber and M_{ac,Mn_i} is accumulated Mn_i removed from the chamber (μg), M_{0,Mn_i} is initial mass of Mn_i in the chamber (μg), and $M_{ac,Mn_{tot}}$ is accumulated total Mn ($Mn_s + Mn_i$) removed from the chamber (μg).

Equation [3] accounts for two processes in the chamber. The first expression (k_4) is the Mn_s source term. Theoretically, Mn_s is inexhaustible, its removal rate is independent of Mn mass, and hence, k_4 is defined as a rate-constant of the zero-order reaction. The second expression (τ_2) is the Mn_s sink term; the rate ($\mu\text{g min}^{-1}$) at which Mn_s discharged out of the chamber. Under the assumption that a SF chamber is a well mixed system (Seyfried et al., 1989), a dilution process occurs in the chamber and τ_2 must be the concentration (ξM_{Mn_s}) multiplied by the flow-rate (Q). Because τ_2 is also the rate at which Mn_s accumulates, Eq. [4] results. The assumption that the SF chamber is well mixed also implies that the rate at which Mn_i is removed from the chamber is equal to its concentration [$\xi (M_{0,Mn_i} - M_{ac,Mn_i})$] multiplied by Q (Eq. [5]). Equation [6] is the sum of Eq. [4] and [5], which is essentially the rate at which total Mn (Mn_{tot}) is removed.

The Mn data were fitted to $dM_{ac,Mn_{tot}}/dt \cdot \Delta t$, where Δt is the time period of collection (Fig. 4). The BMDP AR program (Dixon, 1990) was used for the NLLS fitting. After the data were fitted, the nonobservable components (M_{Mn_s} , $M_{ac,Mn_{tot}}$, M_{ac,Mn_s} , and M_{ac,Mn_i}) were computed using the D02BBF subroutine of NAG to solve the system of ODEs (Eq. [3] through [6]; Numerical Algorithms Group, 1988).

The M_{Mn_i} in the chamber decreased precipitously and then leveled off (Fig. 4). These instantaneously-removed Mn salts immediately entered the solution in the SF chamber upon solution contact. At the same time, the

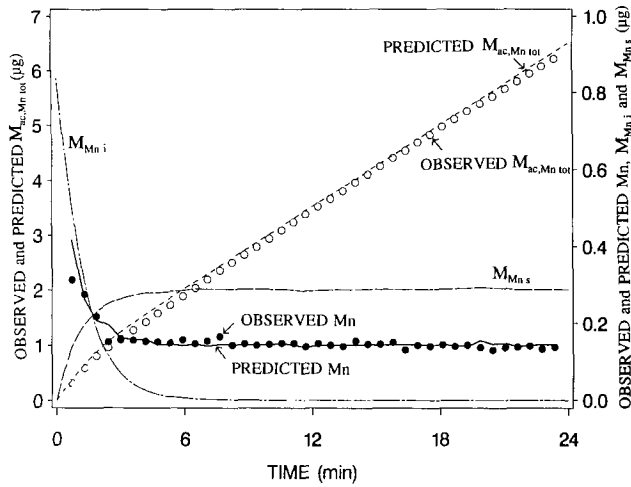


Fig. 4. Measured and predicted Mn mass and its computed components in solution in the SF chamber: M_{Mn_i} is the current mass of indigenous Mn (see definition in the discussion section), M_{Mn_s} is the current mass of Mn that originated from wadginite dissolution, and $M_{ac,Mn_{tot}}$ is the accumulated total Mn ($M_{n_s} + M_{n_i}$) removed from the chamber.

M_{Mn_s} in the chamber increased abruptly and then leveled off. Per given t , M_{Mn_s} in the chamber was higher than the observed Mn because Q restricted the removal rate. After ≈ 4 min, the Mn leveled off, which implied that M_{n_i} was depleted and M_{n_s} reached a steady-state (at $\approx 0.30 \mu\text{g}$).

Estimated parameters for the Mn model, along with their CVs and the pseudo R^2 are given in Table 3. The Mn model prediction of ξ (0.254 mL^{-1}) was in reasonable agreement with the theoretical value of ξ (0.144 mL^{-1}). The estimated value for the rate-constant (k_4 , $0.248 \mu\text{g min}^{-1}$) was verified by multiplying it by the accumulated t (23.4 min); the product ($5.9 \mu\text{g}$) agreed well with the experimental data for accumulated Mn ($6.2 \mu\text{g}$, Fig. 4). The model's predicted value for M_{0,Mn_i} ($0.84 \mu\text{g}$) agreed with $\approx 0.81 \mu\text{g}$ determined from the first three data points (Fig. 4), which accounted for the leaching of easily-removed Mn.

Modeling the Chromium Removal

To model Cr removal, the following setup of ODEs was proposed for the SF system:

$$\frac{dM_{Cr_i}}{dt} = k_5(M_{0,Cr_i} - M_{Cr_i} - M_{ac,Cr_i}) - \tau_4$$

$$M_{Cr_i} = 0 \text{ when } t = 0 \quad [7]$$

Table 3. Theoretical and estimated values for the Mn model in the SF study (Eq. [3]-[6]).†

Parameter	Theoretical	Estimate	Coefficient of variation	Pseudo R^2
ξ , mL^{-1}	0.144	0.254	0.096	0.925
k_4 , $\mu\text{g min}^{-1}$		0.248	0.012	
M_{0,Mn_i} , μg		0.84	0.06	

† ξ is the reciprocal of the volume of the SF chamber; k_4 is the rate-constant for the zero-order reaction of M_{n_s} entering the solution; M_{0,Mn_i} is the initial mass of instantaneously-removed Mn in the chamber.

where $\tau_4 = \xi M_{Cr_i} Q$

$$\frac{dM_{ac,Cr_i}}{dt} = \tau_4 \quad M_{ac,Cr_i} = 0 \text{ when } t = 0 \quad [8]$$

$$\frac{dM_{Cr_s}}{dt} = k_6 - \tau_5 \quad M_{Cr_s} = 0 \text{ when } t = 0 \quad [9]$$

where $\tau_5 = \xi M_{Cr_s} Q$

$$\frac{dM_{ac,Cr_s}}{dt} = \tau_5 \quad M_{ac,Cr_s} = 0 \text{ when } t = 0 \quad [10]$$

$$\frac{dM_{ac,Cr_{tot}}}{dt} = \tau_4 + \tau_5 \quad M_{ac,Cr_{tot}} = 0 \text{ when } t = 0 \quad [11]$$

where t is time (min), M_{Cr_i} is current mass (M) of the rapidly-removed Cr in solution in the chamber (μg), M_{0,Cr_i} is initial mass of Cr_i in the chamber (μg), M_{ac,Cr_i} is accumulated Cr_i removed from the chamber (μg), k_5 is a rate-constant for Cr_i entering the solution (min^{-1}), $\xi = V_{ch}^{-1}$ (0.144 mL^{-1}) in which V_{ch} is volume of the chamber (6.93 mL), Q is flow-rate (mL min^{-1}), M_{Cr_s} is current mass of slowly-removed Cr in the chamber (μg), k_6 is a rate-constant for Cr_s entering the solution ($\mu\text{g min}^{-1}$), M_{ac,Cr_s} is accumulated Cr_s removed from the chamber (μg), and $M_{ac,Cr_{tot}}$ is accumulated total Cr ($Cr_i + Cr_s$) removed from the chamber (μg).

Equation [7] accounts for two processes in the chamber. The first expression is the Cr_i (exhaustible) source term; the rate at which Cr_i is coming into solution. This rate depends on Cr_i mass and therefore, k_5 is a rate-constant for the first-order reaction. The second expression (τ_4) is the Cr_i sink term; the rate ($\mu\text{g min}^{-1}$) at which Cr_i is discharged out of the chamber. The expression τ_4 is equivalent to τ_3 , and the term τ_5 mentioned below, is equivalent to τ_2 . Under the assumption that a SF chamber is a well mixed system, τ_4 and τ_5 must be the concentrations (ξM_{Cr_i} and ξM_{Cr_s}) multiplied by the Q . Because the rates τ_4 and τ_5 are also the rates at which Cr_i and Cr_s accumulate, Eq. [8] and [10] result. Equation [9] also accounts for source-sink processes in the chamber. The source term (k_6) is a rate-constant ($\mu\text{g min}^{-1}$) of the zero-order reaction at which Cr_s is coming into solution. The sink term (τ_5) is the rate ($\mu\text{g min}^{-1}$) at which Cr_s is removed from the chamber. Equation [11] is the sum of Eq. [8] and [10] which is essentially the rate at which total Cr (Cr_{tot}) is removed.

The Cr data were fitted to $dM_{ac,Cr_{tot}}/dt \Delta t$, where Δt is the time period of collection (Fig. 5). The BMDP AR program (Dixon, 1990) was used for the NLLS fitting. After the data were fitted, the nonobservable components (M_{Cr_i} , M_{ac,Cr_i} , M_{Cr_s} , and M_{ac,Cr_s}) were computed, using the D02BBF subroutine of NAG to solve the system of ODEs (Eq. [7] through [11]; Numerical Algorithms Group, 1988).

The model simulated the rapid removal of the Cr_i fraction in the first 4.2 min (Fig. 5). It also showed that the Cr_s ascended sharply in the first 6.6 min and then leveled off. Because of the asymmetry between the relative weight of the Cr_i data (7 data points) and the following tail that resulted from the Cr_s fraction (33 data points),

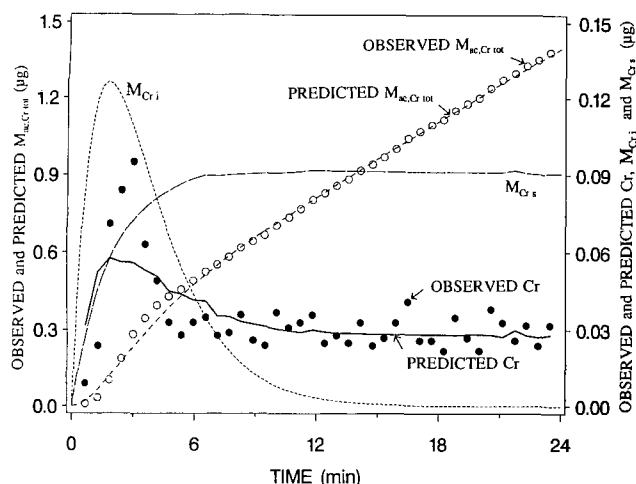


Fig. 5. Measured and predicted Cr mass and its computed components in solution in the SF chamber: M_{Cr_i} is the current mass of desorbed Cr, M_{Cr_s} is the current mass of Cr that may have originated from chromite dissolution, and $M_{ac,Cr,tot}$ is the accumulated total Cr ($Cr_i + Cr_s$) removed from the chamber.

the predicted Cr did not agree with the data through the first 4.2 min. The pseudo R^2 for the Cr model was therefore relatively low (0.51, Table 4). After 4.2 min the observed Cr began to level off, because most Cr_i was virtually depleted and the Cr_s achieved a steady-state (at $\approx 0.09 \mu\text{g}$).

Estimated parameters for the Cr model, along with the pseudo R^2 value for the fit are given in Table 4. The Cr model estimate of ξ (0.157 mL^{-1}) agreed well with the theoretical value of ξ (0.144 mL^{-1}). The predicted value for M_{0,Cr_i} ($0.33 \mu\text{g}$) was agreeable with $\approx 0.40 \mu\text{g}$, determined from the experimental data collected in the first ≈ 4.2 min (Fig. 5), which accounted for the removal of Cr_i . The predicted value for k_6 was validated by subtracting the experimental data for Cr_i ($\approx 0.40 \mu\text{g}$) from the total accumulated Cr data ($1.38 \mu\text{g}$) and dividing it by the time needed for Cr_s to be removed (23.45 min). The quotient ($0.042 \mu\text{g min}^{-1}$) was in good agreement with the model's evaluation for k_6 ($0.048 \mu\text{g min}^{-1}$).

DISCUSSION

Manganese

Both column and SF studies of the Mn removal dynamics showed that instantaneous (relative to the time scale of the major ion release processes) and continuous removal processes occurred. The source for the instantaneously-

Table 4. Theoretical and estimated values for the Cr model (Eq. [7] through [11]).†

Parameter	Theoretical	Estimate	Pseudo R^2
ξ , mL^{-1}	0.144	0.157	0.51
M_{0,Cr_i} , μg		0.33	
k_5 , min^{-1}		0.56	
k_6 , $\mu\text{g min}^{-1}$		0.048	

† ξ is the reciprocal of the volume of the SF chamber; k_5 is the rate-constant for the first-order reaction of Cr_i entering the solution; k_6 is the rate-constant for the zero-order reaction of Cr_s entering the solution; M_{0,Cr_i} is the initial mass of Cr_i in the chamber.

removed Mn (Mn_i) was depleted, whereas the origin of the continuously-removed Mn (Mn_s) was (theoretically, in our model) inexhaustible and steady-state was attained with Mn_s by a replenishment reaction. The question was what were the mechanisms that governed the Mn removal rates.

Both column (Eq. [1]) and SF (Eq. [3]–[6]) models indicated that dilution was the dominant process at the instantaneous-removal stage [$\approx 1.8 \rho$ in the column (Fig. 3) and 3.6 min in the SF (Fig. 4)]. In the column study, the instantaneously-removed fraction (Mn_i) was introduced to the eluent immediately upon wetting of the dry IRM, and it was leached out at a rate governed by the water conductivity in the column. The constant, k_3 , was primarily restricted by the transport-controlled phenomena that predominated in the columns (Salingar et al., 1994a). In the SF study, Mn_i was discharged out of the chamber instantaneously at a rate (τ_3) governed by the dilution process in the chamber, and no time-limiting chemical reactions were involved. Hence, the Mn_i fraction was apparently indigenous Mn salts. These salts were originally released from the solid phase during the IRM generating industrial process and then, after drying the filter-cake, they remained on its surface.

There are two possible mechanisms for the replenishment reaction that sustained the steady-state with respect to Mn_s [at $\approx 48 \mu\text{g L}^{-1}$ in the column (Fig. 3), and at $0.3 \mu\text{g}$ in the SF study (Fig. 4)]: (i) desorption and (ii) dissolution. Both the column and the SF Mn models implied that Mn_s was infinite, and the SF kinetics model indicated that Mn_s that entered the solution could have been controlled through a zero-order reaction (with a rate-constant k_4). Therefore, a dissolution (of, most probably, wadginite) and not a desorption reaction controlled the release of Mn. Similar results were obtained by Krishnamurti and Huang (1988) who found that by introducing Cl solutions, selected Mn-oxide minerals released substantial amounts of Mn, and the removal was rapid initially and then decreased, following multiple zero-order kinetics.

Chromium

The SF Cr model implied that the Cr_i fraction was a finite source. The Cr_i fraction was introduced to the solution rapidly (but not instantaneously like Mn_i) via a first-order reaction, removed from the chamber at a rate that was a function of the dilution process in the chamber, and then depleted. The Cr_s fraction, on the other hand, was fed by a (theoretically) infinite source, and after 6.6 min a steady-state was achieved.

Based on deductions for Cr analogous to those for Mn, the SF kinetics study may indicate that the source for the continuously-removed fraction (Cr_s) is a zero-order dissolution reaction of chromite. Within 6.6 min, a steady-state was attained in the chamber where, most probably, chromite replenishes the solution with Cr.

The source for the rapidly-removed fraction (Cr_i) was depleted within 4.2 min. Yet, in contrast to Mn_i , the Cr_i removal reaction was first-order with a rate-constant (k_5) of 0.56 min^{-1} . It appeared that the Cr_i , which was

originally removed from the solid phase during the IRM generating industrial process, was resorbed by the filter-cake, and then was desorbed via the SF eluent. We assumed that the Cr resorption caused the parabolic behavior observed in the columns.

CONCLUSIONS

Instantaneous and continuous Mn removal processes occurred in the IRM column and SF studies. Volume-dependent dilution of indigenous Mn salts was dominant for the former process whereas dissolution of, most probably, wadginite controlled the zero-order replenishment reaction which sustained the continuous Mn removal process.

Rapidly and continuously removed Cr fractions were also observed. A fraction of the Cr, which was originally removed from the solid phase during the IRM generating industrial process, was re-adsorbed by the filter-cake. This fraction was rapidly removed via a first-order reaction. The source for the continuously removed Cr fraction was apparently a zero-order dissolution reaction of chromite.

Little has appeared in the literature on Mn and Cr removal from high-Fe wastes. The chemistry of Mn and Cr minerals has been extensively studied because these metals are central to a number of economically and environmentally important topics.

This study constitutes part of a comprehensive procedure for examining the environmental soil chemistry of waste products with potential agricultural uses. The results can contribute to rational decisions concerning the proper utilization of the waste product. The proportion of total soluble Mn and Cr in this study was small and therefore, the IRM under investigation may be suitable for agricultural uses under controlled management.

ACKNOWLEDGMENTS

The authors thank the DuPont Company for its support of this research. We also wish to thank Gerald Hendricks for his assistance and Amy Kuchak for her help in the laboratory. Dr. Scott Fendorf is acknowledged for his helpful comments on the manuscript.

REFERENCES

- Amacher, M.C., and D.E. Baker. 1982. Redox involving chromium, plutonium, and manganese in soils. DOE/DP/04515-1. Inst. for Res. on Land & Water Resour., Pennsylvania State Univ., University Park.
- Amacher, M.C., J. Kotuby-Amacher, H.M. Selim, and I.K. Iskandar. 1986. Retention and release of metals by soils—evaluation of several models. *Geoderma* 38:131–154.
- Amacher, M.C., H.M. Selim, and I.K. Iskandar. 1988. Kinetics of chromium(VI) and cadmium retention in soils: A nonlinear multireaction model. *Soil Sci. Soc. Am. J.* 52:398–408.
- Baes, C.F., Jr., and R.E. Mesmer. 1976. The hydrolysis of cations. Wiley Interscience, New York.
- Bartlett, R.J., and B.R. James. 1979. Behavior of chromium in soils: III. Oxidation. *J. Environ. Qual.* 8:31–35.
- Bernas, B. 1968. A new method for decomposition and comprehensive analysis of silicates by atomic absorption spectrometry. *Anal. Chem.* 40:1682–1686.
- Dixon, W.J. (ed.) 1990. Statistical software manual. Vol. 1. Univ. of California Press, Berkeley.
- El-Bassam, N., P. Poelstra, and M.J. Frissel. 1975. Chromium and mercury in a soil after 80 years of treatment with urban sewage water. *Z. Pflanzenernaehr. Bodenk.* 3:309–316.
- Fendorf, S.E., and R.J. Zasoski. 1992. Chromium(III) oxidation by δ -MnO₂. 1. Characterization. *Environ. Sci. Technol.* 26:79–85.
- Fendorf, S.E., M. Fendorf, D.L. Sparks, and R. Gronsky. 1992. Inhibitory mechanisms of Cr(III) oxidation by δ -MnO₂. *J. Colloid Interface Sci.* 153:37–54.
- Goyette, G. 1992. Filter cake (iron-rich) as a component of containerized growth medium and synthetic topsoil. M.S. thesis. Univ. of Delaware, Newark.
- Grove, J.H., and B.G. Ellis. 1980. Extractable chromium as related to soil pH and applied chromium. *Soil Sci. Soc. Am. J.* 44:238–242.
- Griffin, R.A., A.K. Au, and R.R. Frost. 1977. Effect of pH on adsorption of chromium from landfill-leachate by clay minerals. *J. Environ. Sci. Health.* A12(8):431–449.
- JCPDS. 1986. Mineral powder diffraction file. Int. Center for Diffraction Data, Swarthmore, PA.
- Krishnamurti, G.S.R., and P.M. Huang. 1988. Kinetics of manganese released from selected manganese oxide minerals as influenced by potassium chloride. *Soil Sci.* 146:326–334.
- McKenzie, R.M. 1989. Manganese oxide and hydroxides. p. 439–466. In J.B. Dixon and S.B. Weed (ed.) *Minerals in soil environments*. 2nd ed. SSSA Book Ser. 1. SSSA, Madison, WI.
- National Academy of Sciences. 1974. Medical and biological effects of environmental pollutants: Chromium. Committee on biological effects of atmospheric pollutants, Division of Medical Sciences, Nat. Res. Council, Washington, DC.
- Numerical Algorithms Group. 1988. NAG Fortran Library Manual. Mark 13. Vol. 2. NAG, London.
- Rai, D., B.M. Sass, and D.A. Moore. 1987. Chromium(III) hydrolysis constants and solubility of chromium(III) hydroxide. *Inorg. Chem.* 26:345–349.
- Rollinson, C.L. 1973. Chromium, molybdenum and tungsten. p. 623–769. In J.C. Bailar (ed.) *Comprehensive inorganic chemistry*. Pergamon Press, Oxford.
- Sadiq, M. 1981. The adsorption characteristics of soils and sorption of copper, manganese and zinc. *Commun. Soil Sci. Plant Anal.* 12:619–630.
- Saleh, F.Y., T.F. Parkerton, R.V. Lewis, J.H. Huang, and K.L. Dickson. 1989. Kinetics of chromium transformations in the environment. *Sci. Total Environ.* 86:25–41.
- Salingar, Y., D.L. Sparks, and M. Ghodrati. 1994a. Kinetics of ion removal from an iron-rich industrial coproduct: I. Chloride. *J. Environ. Qual.* 23:1194–1200 (this issue).
- Salingar, Y., D.L. Sparks, and J.D. Pesek. 1994b. Kinetics of ion removal from an iron-rich industrial coproduct: II. Sulfate. *J. Environ. Qual.* 23:1201–1205 (this issue).
- Seyfried, M.S., D.L. Sparks, A. Bar-Tal, and S. Feigenbaum. 1989. Kinetics of calcium-magnesium exchange on soil using a stirred-flow reaction chamber. *Soil Sci. Soc. Am. J.* 53:406–410.
- Shuman, L.M. 1977. Effect of soil properties on manganese adsorption isotherms for four soils. *Soil Sci.* 124:77–81.
- Sparks, D.L. 1989. Kinetics of soil chemical processes. Academic Press, New York.
- Stuanes, A. 1976. Adsorption of Mn²⁺, Zn²⁺, Cd²⁺ and Hg²⁺ from binary solutions by mineral material. *Acta Agric. Scand.* 26:243–249.